INTERNATIONAL JOURNAL OF AUTOMOTIVE AND MECHANICAL ENGINEERING (IJAME)
ISSN: 2229-8649 e-ISSN: 2180-1606
VOL. 17, ISSUE 1, 7902 – 7914
DOI: https://doi.org/10.15282/ijame.17.2.2020.09.0590

ORIGINAL ARTICLE

# The Impact of Local Heating Time of the Compressed Column on its Stability

S. Uzny, T. Skrzypczak and L. Kutrowski*

Faculty of Mechanical Engineering and Computer Science, Czestochowa University of Technology, Dabrowskiego 73, 42-201 Czestochowa, Poland. Phone: +48343250679; Fax: +48343250647

**ABSTRACT** – The present paper considers the influence of activity time of a local heat source on the stability of a supporting system (column) subjected to the Euler's external load. Constant heat having impact on the entire circumference of the column on a chosen length was adopted as the boundary heat flux. The formulation and solution of the initial-boundary problem of heat transport in the column was presented by means of the Finite Element Method (FEM). The stiffness of particular segments of the column, onto which it was divided, was determined on the basis of the obtained temporary temperature distributions. The boundary problem of stability of the system was formulated and solved with the inclusion of material changes, resulting from the influence of high temperature. The paper presents the results of numerical simulations, defining the change of a critical load parameter of the system as the function of heating time with the inclusion of stiffness of the supported structure and various positions of the heat flux influence.

**ARTICLE HISTORY**
Revised: 28th Jan 2020
Accepted: 26th Mar 2020

**KEYWORDS**
*Buckling, Heat transfer, Compressive load, Column.*

## INTRODUCTION

The phenomenon of buckling is one of many factors that should be considered when designing slender systems subjected to compressive axial load. The background of these problems is presented in the book [1], where one can find the basics about buckling of eccentric compressed rods, elastic and inelastic buckling of rods, frames and shells. Therein formulations of boundary problems and mathematical models of these systems are presented. Given examples are intended for engineers, constructors and researchers as well as students of technical universities. The typical load, included in the research on stability is the Euler's load, in the case of which the direction of the compressive force is constant and coincides with the direction of the non-deformed axis of the system. The critical load of columns subjected to the Euler's load depends on the manner of mounting. In literature, it is also possible to find other – more complex manners of performing the loading of slender systems, e.g. specific load (generalised with force directed towards a pole [2, 3] or the follower force directed towards a pole [4, 5]).

Due to the wide usage of steel structures as a load-bearing system of storage or production halls, the buckling phenomenon of supports should be included in their design stage as one of the factors that have a significant impact on the load-bearing capacity of the entire system. The document [6] presents the construction requirements pertaining to the calculations regarding steel structures in view of fire design. In a case of fire, the structure is exposed to a high temperature that has an impact on the change of material properties of steel and the development of additional tension. Together with the temperature rise, the value of shear modulus decreases which is connected with lowering the load-bearing capacity of the support system. The analysis of column stability in the case of fire was conducted, inter alia, in many papers. The work [7] includes the study concerning the buckling of beams made of functionally graded materials. Three types of thermal load were considered: uniform temperature rise, linear, and non-linear temperature rise in the cross-section of the column. The results were presented showing critical temperatures of the system with respect to various parameters thereof and the manners of mounting. The publication [8] regards the analysis of buckling of composite columns caused by temperature whose distribution in the cross-section of the system was non-uniform. The considered system was exposed to the heat only from one side. The behaviour of steel columns during a fire was presented in previous work [9]. Considerations were conducted with reference to the buckling moment of the system, its subsequent behaviour and stabilisation. An analytical model and numerical calculations were shown on the basis of the Finite Element Method. The papers [10, 11] cover the analysis of a column subjected to heat load resulting from the damage to the outer protective layer. The model includes the initial column deflection. The impact of the damage to the protective layer on the heating of the system was presented together with its influence on critical load.

Previous works [12, 13] described the phenomenon of elastic and plastic buckling of a steel column, which is pin-connected and subjected to uneven temperature distribution towards the axis of the system. The distribution of temperature was defined in such a manner that allows the determination of two heating zones – warmer in the upper, and cooler in the lower part of the column. The uniform temperature was assumed in the cross-section of the column. The paper [14] adopted a linear distribution of temperature in the cross-section of the column. On the basis of the presented solution, the critical temperature of the system with respect to elastic buckling was sought. Numerical calculations were conducted on the basis of the analytical model and FEM. Three methods of solving differential equations regarding stability with respect to symmetrical laminated composite beams, including various conditions of their mounting, were

*CORRESPONDING AUTHOR | L. Kutrowski | kutrowski@imipkm.pcz.pl

presented in the publication [15]. Dwaikat et al. [16] presented research findings of fire resistance of columns subjected to compressive and bending loads. Results of experimental research on columns having the H cross-section, subjected to heat load, which describe the phenomena of local and global stability loss, can be found in the publication [17].

The aim of this paper is the study of the influence of heating time of the column (subjected to the Euler's external load) on its stability. The presented literature includes the influence of heat on the considered structures, inter alia, through the implementation of various temperature distributions along the system and the occurrence of two heating zones (cooler and warmer). The present paper regards considerations pertaining to the impact of a non-stationary process of heating of a column on its stability. The influence of a heat source on the column is presented in a heating time function. Stability is the main problem that is considered in the following paper, where findings obtained on the basis of a transient process of thermal conduction are used as input. The topic of thermal conduction presented in the paper constitutes a classical issue, however, together with the problem of stability it creates a significant engineering problem within the scope of modelling of slender systems subjected to compressive load. This problem has been intensively developed in recent years, which is demonstrated by numerous publications regarding this area. Due to the fact, there is no link between the two problems presented herein; two parts may be separately distinguished in the present work. The first part includes the formulation of the boundary-initial problem of heat diffusion in the material of the column. On the basis of the adopted initial and boundary conditions, the problem was solved by means of FEM. The obtained temperature distributions were used to determine the stiffness to bending and compressing of particular segments of the column at subsequent moments of heating. The second part of the paper covers the problem of stability, including the changes of properties of column material resulting from temperature rise and the creation of additional loads resulting from thermal expansion of the column material.

## THE BOUNDARY-INITIAL PROBLEM OF HEAT DIFFUSION

Thermal conduction in the steel column with the length of $l$ and diameter $d$ (Figure 1) was described by means of the classical Fourier equation [18], which can be written in the following form:

$$\frac{\partial}{\partial x}\left(\lambda\frac{\partial T}{\partial x}\right)+\frac{\partial}{\partial y}\left(\lambda\frac{\partial T}{\partial y}\right)+\frac{\partial}{\partial z}\left(\lambda\frac{\partial T}{\partial z}\right)=c\rho\frac{\partial T}{\partial t} \tag{1}$$

where $\lambda$ is thermal conduction coefficient (W/mK), $c$ is specific heat (J/kgK), $\rho$ is density (kg/m$^3$), $x$, $y$, $z$ represents Cartesian coordinates (m), $T$ is temperature (K) and $t$ is time (s).

Equation (1) is a mathematical description of a transient process of heat diffusion in the three-dimensional area in the Cartesian coordinates. In order to solve this equation, it should be supplemented with appropriate boundary and initial conditions. As the boundary condition (the Neumann condition) was used in this paper, which defines heat flux $q_b$ in the direction normal to the surface of considered structure:

$$q_b=-\lambda\frac{\partial T}{\partial n} \tag{2}$$

where $n$ means the direction of the vector normal to the surface of the column.

It should be noted that the heat flux from Eq. (2) takes a value greater than zero in the heating zone (column fragment with the length of $h$ shown in Figure 1) and a zero value on the remaining surface of the column. The centre of this zone lies at a distance of $l_l$ from the mount. It was assumed that the heat flux acting on the surface of the column in the heating zone has a constant value. The initial condition takes the form of known initial temperature distribution:

$$T(x,y,z,t=0)=T_0 \tag{3}$$

The solution of Eq. (1) with Eq. (2) and (3) was obtained with the use of FEM which is a very fast and efficient method in the case of parabolic differential equations.

In order to solve Eq. (1) it was initially multiplied by the function $w$ and integrated over the considered volume $\Omega$:

$$\int_\Omega w\left[\frac{\partial}{\partial x}\left(\lambda\frac{\partial T}{\partial x}\right)+\frac{\partial}{\partial y}\left(\lambda\frac{\partial T}{\partial y}\right)+\frac{\partial}{\partial z}\left(\lambda\frac{\partial T}{\partial z}\right)-c\rho\frac{\partial T}{\partial t}\right]d\Omega=0 \tag{4}$$

Then the order of Eq. (4) was lowered and the weak form obtained as Eq. (5):

$$\int_\Omega \lambda\left(\frac{\partial w}{\partial x}\frac{\partial T}{\partial x}+\frac{\partial w}{\partial y}\frac{\partial T}{\partial y}+\frac{\partial w}{\partial z}\frac{\partial T}{\partial z}\right)d\Omega+\int_\Omega wc\rho\frac{\partial T}{\partial t}d\Omega_i=\int_\Gamma wq_b d\Gamma \tag{5}$$

where Γ represents the surface of the column.

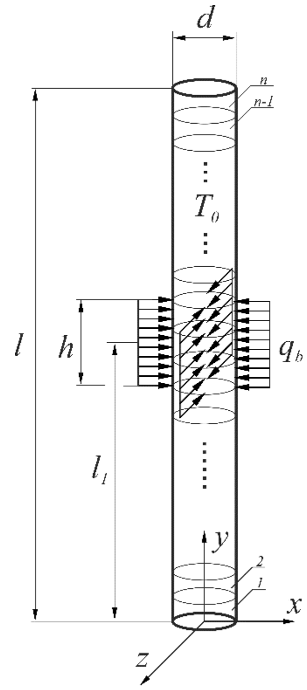


**Figure 1.** Diagram of the system of the heat-loaded column.

The volume of the column was discretised into the set of three-dimensional finite elements. Standard Galerkin formulation was adopted assuming weight functions *w* the same as the shape functions *N* of the finite element:

$$\lambda^{(e)} \int_{\Omega^{(e)}} \left( \frac{\partial N_i}{\partial x} \frac{\partial N_j}{\partial x} + \frac{\partial N_i}{\partial y} \frac{\partial N_j}{\partial y} + \frac{\partial N_i}{\partial z} \frac{\partial N_j}{\partial z} \right) d\Omega^{(e)} T_j^{(e)} + \\ +(c\rho)^{(e)} \int_{\Omega^{(e)}} N_i N_j d\Omega^{(e)} \frac{\partial T_j^{(e)}}{\partial t} = \int_{\Gamma^{(e)}} N_i q_b d\Gamma^{(e)} \tag{6}$$

where ($e$) refers to the finite element, $i, j$=1,2,...,$nn$, $nn$ – is the number of nodes in the element, $N$ – denotes the shape function.

The following integral terms are recognised in Eq. (6):

$$K_{ij}^{(e)} = \lambda^{(e)} \int_{\Omega^{(e)}} \left( \frac{\partial N_i}{\partial x} \frac{\partial N_j}{\partial x} + \frac{\partial N_i}{\partial y} \frac{\partial N_j}{\partial y} + \frac{\partial N_i}{\partial z} \frac{\partial N_j}{\partial z} \right) d\Omega^{(e)} \tag{7}$$

$$M_{ij}^{(e)} = (c\rho)^{(e)} \int_{\Omega} N_i N_j d\Omega^{(e)} \tag{8}$$

$$B_i^{(e)} = \int_{\Gamma^{(e)}} N_i q_b d\Gamma^{(e)} \tag{9}$$

where $K_{ij}^{(e)}$, $M_{ij}^{(e)}$, $B_i^{(e)}$are the elements of the thermal conductivity matrix, heat capacity matrix, and the boundary condition vector of the finite element, respectively.

In regards to Eq. (7) to (9), Eq. (6) is written in the matrix form as in Eq. (10):

$$\boldsymbol{K}^{(e)} T^{(e)} + \boldsymbol{M}^{(e)} \dot{\boldsymbol{T}}^{(e)} = \boldsymbol{B}^{(e)} \tag{10}$$

For the entire column one can write the global matrix equation:

$$\boldsymbol{KT} + \boldsymbol{M}\dot{\boldsymbol{T}} = \boldsymbol{B} \tag{11}$$

In order to perform time discretisation of Eq. (11), a time grid was introduced into the considerations:

$$t_0 < t_1 < \cdots < t^{f-1} < t^f < t^{f+1} < \cdots < t_k \tag{12}$$

Time amount between $t^l$ and $t^{f+1}$ is called the time step:

$$\Delta t = t^{f+1} - t^f \tag{13}$$

The time derivative of temperature was approximated according to the following linear differential scheme:

$$\dot{\boldsymbol{T}} = \frac{\boldsymbol{T}^{f+1} - \boldsymbol{T}^f}{\Delta t} \tag{14}$$

After inserting Eq. (14) into Eq. (11), global set of equations is obtained in the following form:

$$\left(\boldsymbol{K} + \frac{1}{\Delta t}\boldsymbol{M}\right)\boldsymbol{T}^{f+1} = \boldsymbol{B} + \frac{1}{\Delta t}\boldsymbol{M}\boldsymbol{T}^f \tag{15}$$

Equation (15) results from the usage of the Euler backward scheme of the integration with respect to time. It allows the determination of temporary temperature distributions in the subsequent time steps.

The solution of the boundary problem of stability of the system required the division of a column onto $n$ segments (Figure 1). The value of Young's modulus is determined in each time step as the function of temperature according to [6, 19]:

$$\begin{aligned} \frac{E(T_C)}{E(20)} &= 1 + \frac{T_C}{2000\, ln\left(\frac{T_C}{1100}\right)}, \qquad for\ 20°C \le T_C \le 600°C \\ \frac{E(T_C)}{E(20)} &= \frac{690 - 0.69T_C}{T_C - 53.5}, \qquad for\ 600°C \le T_C \le 1000°C \end{aligned} \tag{16}$$

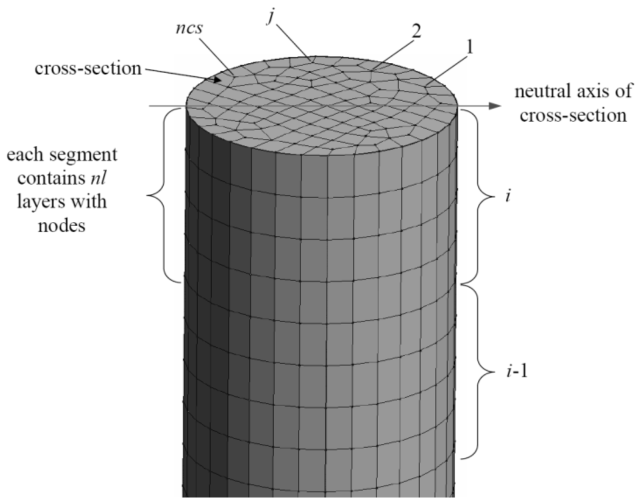


**Figure 2.** Column fragment subjected to spatial discretisation.

The finite element mesh contains a certain number of horizontal layers with nodes (Figure 2). Each layer has the same distribution of nodes. Each horizontal segment of the column comprises $nl$ of such layers. Such a uniform structure of the mesh makes it possible to easily determine stiffness to expansion-compression $(EA)_{cs}$, bending $(EI)_{cs}$ and temperature $T_{cs}$ in every cross-section of the column:

$$(EA)_{cs} = \sum_{j=1}^{n_{cs}} E_j A_j \tag{17}$$

$$(EI)_{cs} = \sum_{j=1}^{n_{cs}} E_j I_j \tag{18}$$

$$T_{cs} = \frac{\sum_{j=1}^{n_{cs}} A_j T_j}{A_{cs}} \tag{19}$$

where $E_j$ - Young's modulus in the $j$-th node of the cross-section, $T_j$ – temperature in the $j$-th node of the cross-section, $A_j$ - partial area of the cross-section of the column assigned to the $j$-th node, $I_j = A_j r_j^2$ - partial moment of inertia assigned to the $j$-th node, $r_j$ - distance of the $j$ node from the neutral axis of the cross-section (the location of the neutral axis depends on the shape of the cross-section and temperature distribution), $ncs$ - the number of nodes in the cross-section of the column, $A_{cs}$ - area of the cross-section of the column.

After the calculation of $(EA)_{cs}$, $(EI)_{cs}$ and $T_{cs}$ in each cross-section of the column, it is possible to average these parameters in the $i$-th segment:

$$(EA)_i = \frac{\sum_{cs=1}^{n_l}(EA)_{cs}}{n_l} \tag{20}$$

$$(EI)_i = \frac{\sum_{cs=1}^{n_l}(EI)_{cs}}{n_l} \tag{21}$$

$$(T)_i = \frac{\sum_{cs=1}^{n_l}T_{cs}}{n_l} \tag{22}$$

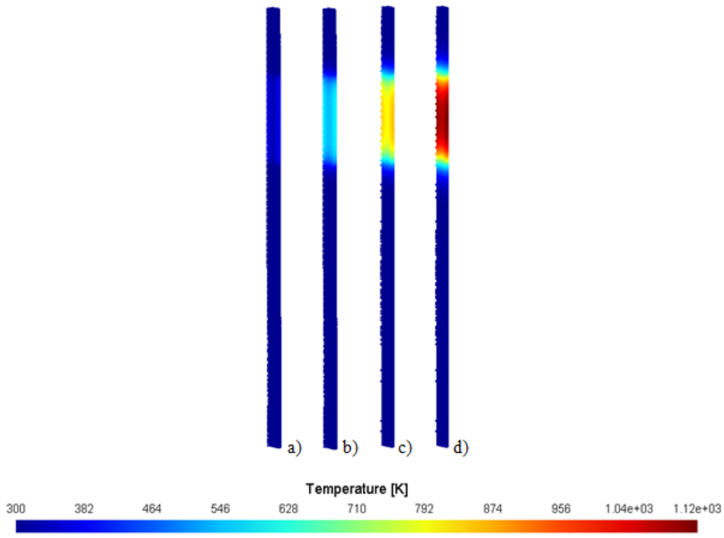


**Figure 3.** Exemplary temporary temperature distributions in the column for (a) $t$=10 s, (b) $t$=50 s, (c) $t$=100 s, and (d) $t$=150 s at system parameters of $d$=0.03 m, $l$=1 m, $l_I$=0.75 m, $q_b$=200000 W/m$^2$, $h$=0.2 m.

Transient process of heat transport results in the evolution of the temperature distribution shown in Figure 3. Determination of averaged parameters (20-22) in every segment of the column was performed in each time step when 293,15 K<$T$<1273,15 K. Such a range of temperature is acceptable for Eq. (16). Finally the calculated parameters (20-22) were saved in the text files for the boundary problem of the column stability which is the next part of solution.

## THE BOUNDARY PROBLEM OF SYSTEM STABILITY

The schemes of the considered systems were presented in Figure 4. The column with the length of $l$ is subjected to compressive force $P$ (force $P$ is characterised by constant direction of activity during the deflection of the system (Euler force)) and the local heat source. In the present paper, the considered column serves as a support, maintaining the structure of a given stiffness. For this reason, a translational spring with the stiffness of $K_{T1}$, having longitudinal direction to the axis of the column, may be found at the loaded end of the system. This spring models the stiffness of the supported structure in the $x$ direction. Two cases of system mounting are considered $E1$ (Figure 4(a)) and $E2$ (Figure 4(b)). In the first case ($E1$), there is no possibility of rotation and translation in the $x$ direction in the places of column mounting. In the latter ($E2$), there is a possibility of rotation of its loaded end. The considered column is a continuous system, divided into segments. The division into segments was conducted in order to obtain the distribution of material properties along the column, which are significantly dependent on temperature.

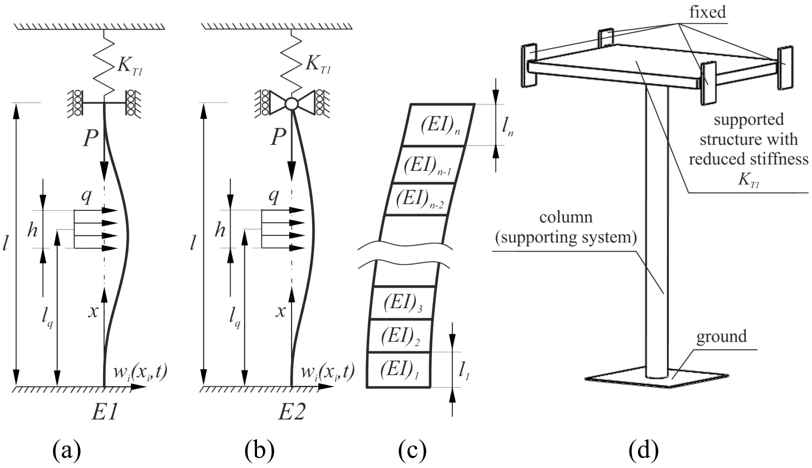


**Figure 4.** The scheme of the column subjected to the Euler's load and local heat source: (a) column E1, (b) column E2, (c) column divided into segments and (d) representation of the real system.

The formulation of the boundary problem of stability of the system is conducted on the basis of the principle of minimum potential energy:

$$\delta V = 0 \tag{23}$$

Potential energy $V$ of the considered system may be written in the following form:

$$V = \frac{1}{2}\sum_{i=1}^{n}\int_0^{l_i}(EI)_i\frac{d^2w_i(x_i)}{dx_i^2}dx_i + \frac{1}{2}\sum_{i=1}^{n}\int_0^{l_i}(EA)_i\left\{\begin{matrix}\frac{du_i(x_i)}{dx_i}+\frac{1}{2}\left(\frac{dw_i(x_i)}{dx_i}\right)^2+\\-\alpha_i\Delta T_i\end{matrix}\right\}^2 dx_i + \\ +\frac{1}{2}K_{T1}u_n(l_n)^2 + Pu_n(l_n) \tag{24}$$

where: $(EI)_i$, $(EA)_i$ - stiffness to bending and compression of the $i$ segment of the column, $w_i(x_i)$, $u_i(x_i)$ – displacement of the $i$ segment of the column in the transverse and longitudinal direction corresponding to the coordinate $x_i$, $A_i$ – cross-section area of the $i$ segment of the column, $\alpha_i$ – temperature expansion coefficient of the $i$ segment of the column, $K_{T1}$ – stiffness of the spring modelling the stiffness of the supported structure in the longitudinal direction with respect to the non-deformed axis of the column , $\Delta T_i$ – temperature rise of the $i$ segment of the column.

On the basis of the model (23), system displacement equations are obtained in the transverse and longitudinal direction to the non-deformed axis of the column:

$$(EI)_i\frac{d^4w_i(x_i)}{dx_i^4} + S_i\frac{d^2w_i(x_i)}{dx_i^2} = 0 \tag{25}$$

$$\frac{d}{dx_i}\left\{\frac{du_i(x_i)}{dx_i}+\frac{1}{2}\left(\frac{dw_i(x_i)}{dx_i}\right)^2 - \alpha_i T_i\right\} = 0 \tag{26}$$

The inner force in the segment is, by definition, equal to:

$$S_i = -(EA)_i\left(\frac{du_i(x_i)}{dx_i}+\frac{1}{2}\left(\frac{dw_i(x_i)}{dx_i}\right)^2 - \alpha_i T_i\right) \tag{27}$$

It is assumed that between the subsequent segments, deflections and deflection angles are equal together with the equality of longitudinal displacements:

$$w_i(l_i) - w_{i+1}(0) = 0 \tag{28}$$

$$\left.\frac{dw_i(x_i)}{dx_i}\right|^{x_i=l_i} - \left.\frac{dw_{i+1}(x_{i+1})}{dx_{i+1}}\right|^{x_i=0} = 0 \tag{29}$$

$$u_i(l_i) - u_{i+1}(0) = 0 \tag{30}$$

By including Eq. (28) and (29) in the variation of potential energy, other conditions of system continuity between particular segments are obtained:

$$(EI)_i \frac{d^2 w_i(x_i)}{dx_i^2}\bigg|^{x_i=l_i} - (EI)_{i+1} \frac{d^2 w_{i+1}(x_{i+1})}{dx_{i+1}^2}\bigg|^{x_i=0} = 0 \tag{31}$$

$$-(EI)_i \frac{d^3 w_i(x_i)}{dx_i^3}\bigg|^{x_i=l_i} + (EI)_{i+1} \frac{d^3 w_{i+1}(x_{i+1})}{dx_{i+1}^3}\bigg|^{x_i=0} = 0 \tag{32}$$

The boundary conditions of the considered column in the longitudinal direction may be written as follows:

$$u_1(0) = 0 \tag{33}$$

$$S_n - K_{T1} u_n(l_n) - P = 0 \tag{34}$$

Boundary conditions connected with the ends of the column ($x_1$=0 and $x_n$=$l_n$) in the transverse direction depend on the manner of mounting. These conditions are given in Table 1.

**Table 1.** Boundary conditions of the column in the transverse direction.

| E1 (Figure 4(a)) | | E2 (Figure 4(b)) | |
|---|---|---|---|
| $w_1(0) = 0$ | (35a) | $w_1(0) = 0$ | (36a) |
| $\frac{dw_1(x_1)}{dx_1}\Big\|^{x_1=0} = 0$ | (35b) | $\frac{dw_1(x_1)}{dx_1}\Big\|^{x_1=0} = 0$ | (36b) |
| $w_n(l_n) = 0$ | (35c) | $w_n(l_n) = 0$ | (36c) |
| $\frac{dw_n(x_n)}{dx_n}\Big\|^{x_n=l_n} = 0$ | (35d) | $\frac{d^2 w_n(x_n)}{dx_n^2}\Big\|^{x_n=l_n} = 0$ | (36d) |

Due to the occurrence of non-linearity, in order to conduct the final formulation of the boundary problem of stability, the following substitutions are introduced into differential equations and boundary conditions ($\varepsilon$ is the small parameter of the deflection of the system):

$$w_i(x_i) = \varepsilon w_{i1}(x_i) \tag{37}$$

$$S_i = S_{i0} \tag{38}$$

$$u_i(x_i) = u_{i0}(x_i) \tag{39}$$

By grouping expressions with the same power $\varepsilon$ ($\varepsilon^0$ and $\varepsilon^1$) two equations were obtained:

$$\varepsilon^0 : \frac{d}{dx_i}\left\{\frac{du_{i0}(x_i)}{dx_i} - \alpha_i T_i\right\} = 0 \tag{40}$$

$$\varepsilon^1 : (EI)_i \frac{d^4 w_{i1}(x_i)}{dx_i^4} + S_{i0} \frac{d^2 w_{i1}(x_i)}{dx_i^2} = 0 \tag{41}$$

After two integrations of Eq. (40) and after inclusion of longitudinal displacement continuity on the boundary of the segments, it is possible to write down the final form of equations regarding longitudinal displacements of particular column elements:

$$u_{i0}(x_i) = \sum_{j=1}^{i-1}\left(-\frac{S_{j0} l_j}{(EA)_j} + \alpha_j T_j l_j\right) - \frac{S_{i0} x_i}{(EA)_i} + \alpha_i T_i x_i \tag{42}$$

After conducting mathematical transformations, with the usage of appropriate boundary conditions, an equation was obtained through which the values of inner forces are determined in the subsequent segments of the system:

$$S_{i0} = \frac{K_{T1} \sum_{i=1}^{n} \alpha_i T_i l_i + P}{1 + K_{T1} \sum_{i=1}^{n} \frac{l_i}{(EA)_i}} \tag{43}$$

$$S_i = S_{i+1} \tag{44}$$

The solution of Eq. (25) maybe written in the form of:

$$w_i(x_i) = A_i\cos(k_i x_i) + B_i\sin(k_i x_i) + C_i x_i + D_i;\ \text{ where } k_i = \left(\frac{S_{i0}}{(EI)_i}\right)^{\frac{1}{2}} \tag{45}$$

After including the conditions of given dependencies 28, 29, 31 and 32 and appropriate conditions connected with transverse displacements 35 or 36 (conditions 35 correspond to the mounting *E1* and 36 to the mounting *E2*), a system of equations is obtained whose matrix determinant of coefficients equated to zero is a transcendental equation, used to determine the critical load of the system. The determined critical load may be used to load the system at a given moment of heating. The bisection method is used in the algorithm for determine the next roots of the determinant function [20].

## RESULTS OF NUMERICAL CALCULATIONS

Numerical calculations were conducted in two stages. The first covered the solution of the thermal conduction problem. In order to achieve this aim, an original solver was used that is based on solving differential equations using the finite element method. On the basis of the obtained temperature distributions, stiffnesses to bending and compressing were determined with respect to particular segments of the column at the subsequent moments of its heating. The detailed determination method of stiffnesses to bending and compressing of particular segments of the system is presented earlier in the paper. The second stage of numerical calculations covers the boundary problem of stability where the maximum load that may have an impact on the system was determined. In order to present the obtained results of numerical calculations, non-dimensional parameters were introduced as follows:

$$\zeta_p = \frac{P_{cr} l^2}{(EI)_{T0}} \tag{46}$$

$$k_{T1} = \frac{K_{T1} l^3}{(EI)_{T0}} \tag{47}$$

$$\zeta_q = \frac{l_q}{l} \tag{48}$$

$$\zeta_h = \frac{h}{l} \tag{49}$$

where: $\zeta_p$ – parameter of critical load of the system, $k_{T1}$ – stiffness parameter of the translational spring in the longitudinal direction to the non-deformed axis of the system, $\zeta_q$ – location parameter of the local heat source, $\zeta_h$ – height parameter of the local heat source, $(EI)_{T0}$ – stiffness to bending of the column not exposed to heat.

The present paper studies the influence of stiffness of the supported structure (impact of the translational spring stiffness $k_{T1}$) and the location of the local heat source on the stability of the considered system. Calculations were conducted with constant length of the column $l$=1 m, constant value of the heat flux $q$=200000 W/m$^2$,
constant height of the heat flux $h$=0.2 m, two manners of column mounting *E1* and *E2*, at three locations of the local heat source $\zeta_q$= {0.25, 0.5, 0.75}, stiffnesses of the supported system (curves presented in the diagrams (Figure 5 to Figure 14) correspond to the values of the stiffness parameter $k_{T1}$): 1. $k_{T1}$=0; 2. $k_{T1}$=25000; 3. $k_{T1}$=50000; 4. $k_{T1}$=75000; 5. $k_{T1}$=100000; 6. $k_{T1}$=125000; 7. $k_{T1}$=150000; 8. $k_{T1}$=175000; 9. $k_{T1}$=200000, support diameter $d$= {0.01, 0.015, 0.02, 0.025, 0.03} m.

The presented findings do not include the behaviour of the system within the plastic range (beyond the yield strength). Due to this fact, the presented dependencies of load in the heating time function of the column should be limited in each case to the value of yield strength of the considered material.

### Mounting *E1* (cf. Figure 4)

In Figure 5 to Figure 9, dependencies between the parameter of external critical load of the column $\zeta_p$ and the time of its heating $t$, were presented at various values of the parameter $k_{T1}$. The figures refer to different diameters of the support and the diagrams in these figures regard different places of heating (*a* and *b*). In the case of the column *E1*, due to its symmetry against the centre, only two locations of the heat source $\zeta_q$={0.75, 0.5} are taken into account. Results for the location $\zeta_q$={0.25, 0.75} are the same.

When the diameter of the support are smaller, and the stiffness of the supported system is higher, the considered changes of the external parameter of critical load have an almost linear character. Depending on the stiffness of the supported system (stiffness $k_{T1}$), a different rate of change of the considered critical load is obtained. When the diameters of the support are $d$={0.01, 0.015, 0.02, 0.025} m and with two locations of the heat source, it was observed that there is heating time in which the stiffness of the supported system does not have an impact on critical load. The considered curves intersect at one point (cf. point $S_1$). If $d$=0.03 m, this characteristic point occurs when $\zeta_q$=0.5. When the $\zeta_q$=0.75, the intersection point of curves does not exist. When the diameters of the support are larger ($d$={0.025, 0.03} m), it was observed that by heating the system for a longer period of time, an increase of critical load is obtained together with heating time. It is especially noticeable in the case when $\zeta_q$=0.75. This phenomenon is caused by the fact that when the temperatures of the column are higher, its stiffness to compressing is decreasing, which in turn causes the decrease of the inner force. The external force loading the entire system is divided into two components: the force carried by the support (inner force – $S_{i0}$ (Eq. (43))) and the force carried by the supported system, whose stiffness is determined by the parameter $k_{T1}$.

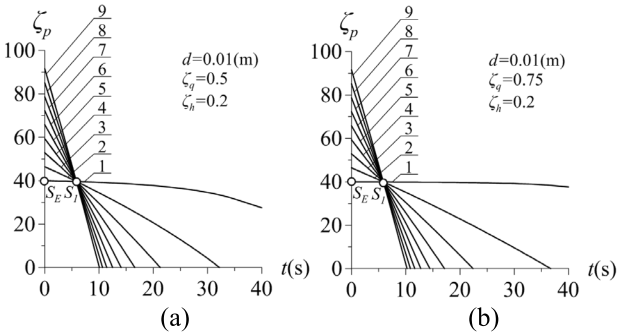


**Figure 5.** The impact of the parameter $k_{T1}$ on the critical load of the column with the diameter of $d$=0.01 m: (a) $\zeta_q$=0.5; (b) $\zeta_q$=0.75.

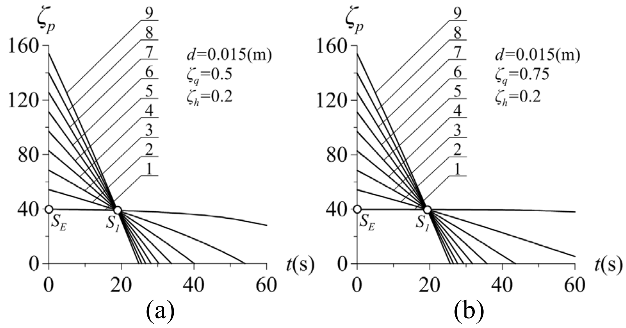


**Figure 6.** The impact of the parameter $k_{T1}$ on the critical load of the column with the diameter of $d$=0.015 m: (a) $\zeta_q$=0.5; (b) $\zeta_q$=0.75.

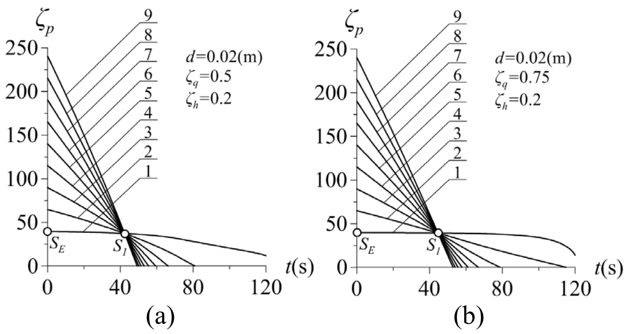


**Figure 7.** The impact of the parameter $k_{T1}$ on the critical load of the column with the diameter of $d$=0.02 m: (a) $\zeta_q$=0.5 and (b) $\zeta_q$=0.75.

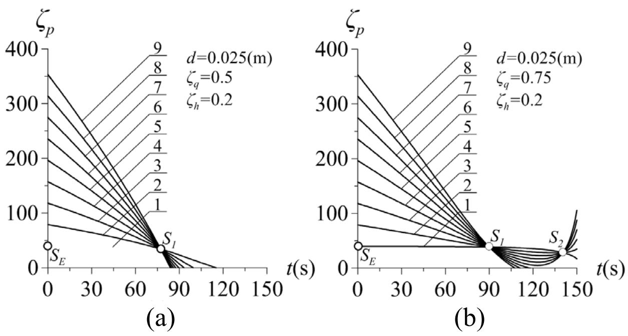


**Figure 8.** The impact of the parameter $k_{T1}$ on the critical load of the column with the diameter of $d$=0.025 m: (a) $\zeta_q$=0.5 and (b) $\zeta_q$=0.75.

On the other hand, the stiffness of the non-heated fragments of the column with larger diameters is big enough to cause the increase of external critical load that has an impact on the entire system (the increase is presented in Figure 9). Additionally, by heating the column from a close distance from the rigid mounting, there is a smaller impact of support stiffness decrease on its load-bearing capacity in comparison to the central placement of the heat source. In the case of the diameter $d$=0.025 m, the occurrence of a second characteristic point was observed, where curves corresponding to the stiffness parameters $k_{T1}$={0, 25000, 50000, 75000, 100000, 125000} intersect.

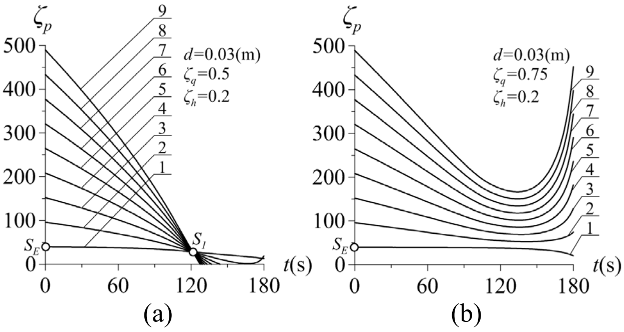


**Figure 9.** The impact of the parameter $k_{T1}$ on the critical load of the column with the diameter of $d$=0.03 m: (a) $\zeta_q$=0.5 and (b) $\zeta_q$=0.75.

### Mounting *E2* (cf. Figure 4)

The results presented in this subparagraph refer to the column mounting *E2* shown in Figure 4(b). In the case of the considered mounting, due to its asymmetry against the centre of the column, three different placements of the heat source $\zeta_q$={0.25, 0.5, 0.75} were included. As in previous cases, calculations were conducted with respect to five diameters of the column $d$={0.01, 0.015, 0.02, 0.025, 0.03} m and various stiffnesses of the supported system. In all considered cases, there is a heating time during which the analysed stiffness of the supported system does not have an impact on the critical load of the column. The considered curves, with respect to critical load – heating time, intersect at one point (point $S_I$). When the heating time is shorter in comparison to the time determined by the point $S_I$, an increase of the stiffness of the supported system also increases the external critical load. While taking into account longer heating time, an increase of stiffness of the supported system decreases the critical load. The increase of the diameter of the supporting system (column) increases the critical load of the system and extends the heating time corresponding to the point $S_I$. In the case of the mounting *E2* (in the analysed scope of the adopted diameters), there was no increase of critical load together with the heating time as in the system *E1*. The critical load corresponding to the point $S_I$ (the point of intersection of the considered curves) is close to the critical load of the column subjected only to the external load (Euler critical force – point $S_E$) without the inclusion of the load resulting from heating. The curve connected with the zero-stiffness of the supported system over a period of heating time from zero till the time corresponding to the point $S_I$ is almost horizontal. This regularity occurs both in the system *E1* and *E2*.

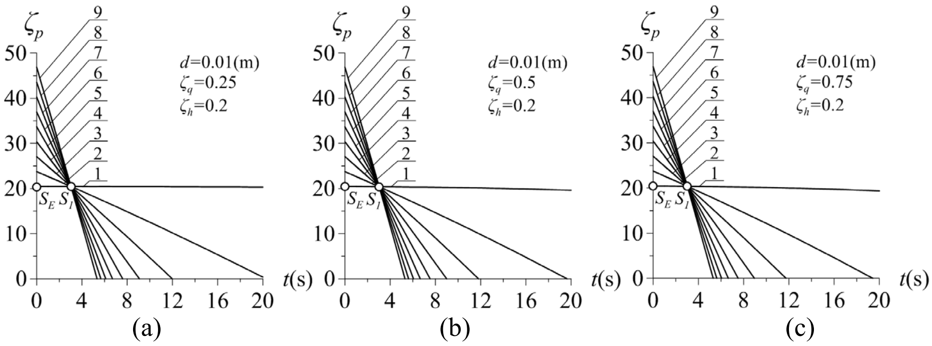


**Figure 10.** The impact of the parameter $k_{T1}$ on the critical load of the column with the diameter of $d$=0.01 m: (a) $\zeta_q$=0.25, (b) $\zeta_q$ =0.5 and (c) $\zeta_q$ =0.75.

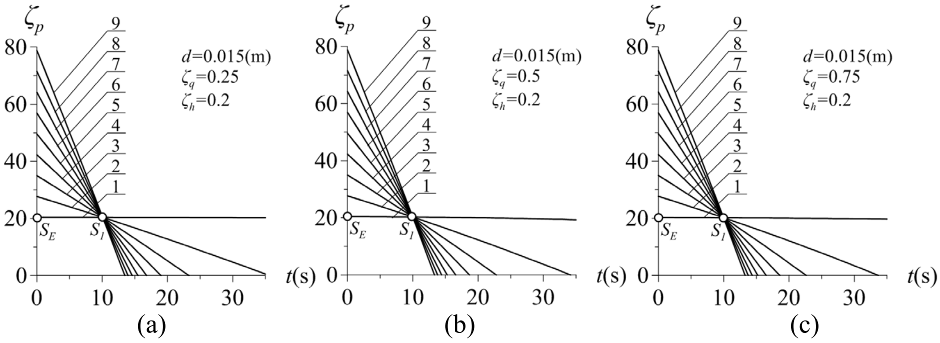


**Figure 11.** The impact of the parameter $k_{T1}$ on the critical load of the column with the diameter of $d$=0.015 m: (a) $\zeta_q$=0.25, (b) $\zeta_q$ =0.5 and (c) $\zeta_q$ =0.75.

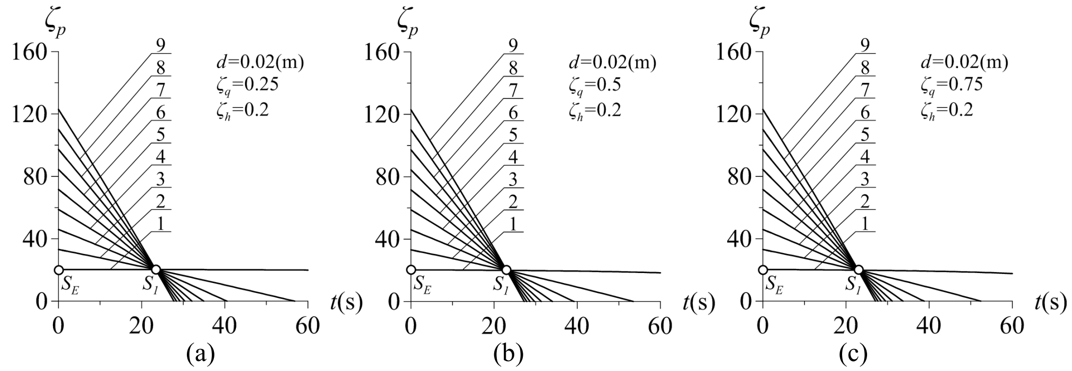


**Figure 12.** The impact of the parameter $k_{T1}$ on the critical load of the column with the diameter of $d$=0.02 m: (a) $\zeta_q$=0.25, (b) $\zeta_q$ =0.5 and (c) $\zeta_q$ =0.75.

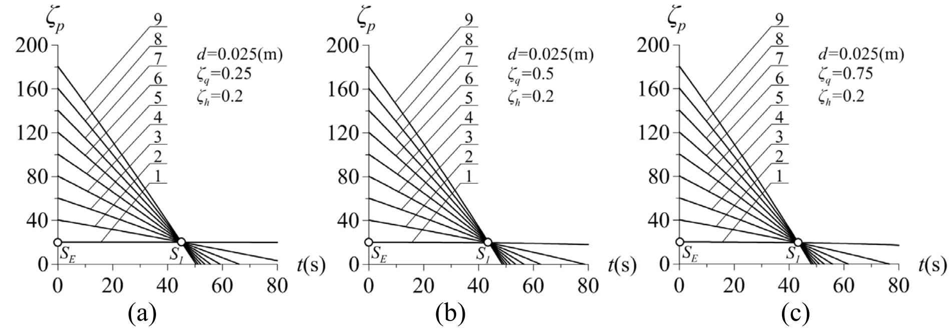


**Figure 13.** The impact of the parameter $k_{T1}$ on the critical load of the column with the diameter of $d$=0.025 m: (a) $\zeta_q$=0.25, (b) $\zeta_q$ =0.5 and (c) $\zeta_q$ =0.75.

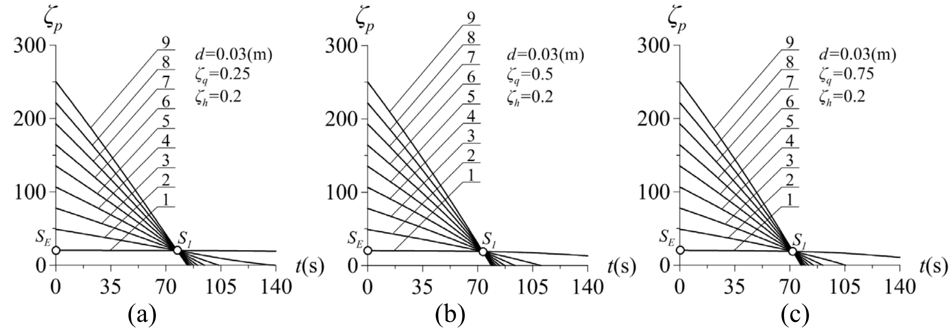


**Figure 14.** The impact of the parameter $k_{T1}$ on the critical load of the column with the diameter of $d$=0.03 m: (a) $\zeta_q$=0.25, (b) $\zeta_q$ =0.5 and (c) $\zeta_q$ =0.75.

The present paper shows the critical force values with which the system may be loaded, and this system is subjected to the additional impact of the external heat source. Therefore, a critical case is being considered. The intersections of curves at $S_1$ and $S_2$ points result from the evenness of system reduction (caused by the impact of the external compressive force) and extension (caused by thermal expansion of column material). In work [9], Shepherd and Burgess obtained the results of numerical calculations of the internal force in a column in the temperature function, depending on the restrain ratio, with a considered constant external axial load, lower than the critical load. Figure 15 presents the change of axial displacement of the column end in the case where the connection ($E1$) was chosen, depending on the time of system heating. It was proven that for the subsequent diameters of the column, the $S_1$ and $S_2$ intersection points of curves correspond to the zero value of $u_n(l_n,t)$ longitudinal displacement.

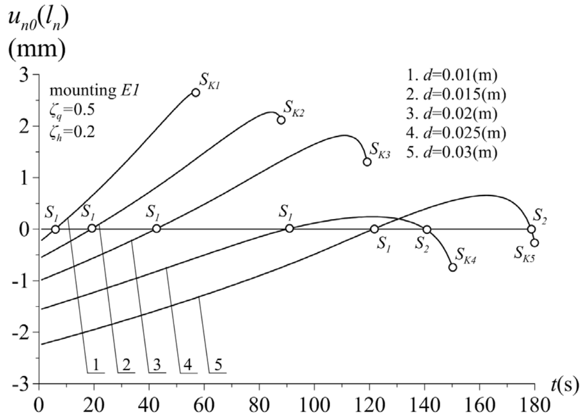


**Figure 15.** Longitudinal displacement of the loaded end of the system $u_{n0}(l_n)$ in the heating time function.

In the case where the heating time is shorter than the one that corresponds to the $S_1$ point, the reduction of the column length under the influence of external force is greater than the extension caused by thermal expansion. At the $S_1$ point, the reduction of external force is equal to the extension through thermal expansion, which corresponds to the zero longitudinal displacements of the loaded end (cf. [9]). The continuation of column heating causes an increase with respect to the extension. It also occurs until a certain moment of heating (the time between the point $S_1$ and $S_2$), which corresponds to the extreme (maximum) of the considered curves. After the extreme is reached, the extension is reduced as a result of heating. It is caused by a significant loss of stiffness to compression. At the $S_2$ point, the longitudinal displacement of the loaded end of the considered column reaches the zero value again. The final time of column heating is connected with reaching the maximum temperature with respect to which it is possible to determine Young's modulus on the basis of appropriate equations available in the literature [6, 19]. In the case of systems having smaller diameters, this time is shorter in comparison to the columns characterised by greater diameters (Figure 15 – $S_{ki}$ points).

Our results show a good correlation with results obtained by other researchers, that are commonly considered in the temperature domain. However, other papers most often presented results in the field of temperature. Given the fact that the increase in exposure time to a heat source relates to an increase in temperature, a comparison of results can be made on this basis. The relations contained in Figure 5 to Figure 14 can be compared with the results of the work [9], which describes the relationship between the force generated in the system and the temperature for various restrain ratios. Data were presented in the buckling and post-buckling range. In our work the buckling results are presented on the plane of critical load - heating time. The heating up time is the same as the temperature increase, whereas the relationship between the force (cf. [9]) and the critical load is inverse. In work [9], the load generated in the system was analysed against increasing temperature. In contrast, our approach deliberates the maximum critical load of the support system, together with the increase of exposure time due to the heat source. When the temperature (or the time of exposure to the heat source) increases, the force generated in the system increases, while the critical load decreases. Both analyses conclude proportional gradient of the curves for increasing stiffness (restrain ratio and $K_{T1}$). Furthermore, a similar characteristic point of intersection of the curves can be seen.

Our calculations of the relationship between the displacement of the column's end and the heating time (cf. Figure 15) is in good agreement with numerical solutions shown in [9-11] and the results of experimental research described in [16].

## CONCLUSION

The work presents the results of numerical calculations of the impact of the longitudinal stiffness parameter of the translational spring (modelling the stiffness of the supported system) on column stability. Two cases of column mounting were considered: a column rigidly fixed at both ends as well as rigidly fixed at the lower and pin-connected at the upper part thereof.

Numerical calculations were conducted with respect to various diameters of the considered columns. Based on the presented results, it is possible to determine the extent of changes of critical load in the function of heating time of the support. It was found that the stiffness of the supported system has a great influence on the stability of the supporting structure (column). Findings of this type of research are significant when the strength of a structure exposed to fire is considered. Moreover, based on the obtained dependencies, it is possible to determine parameters that increase or decrease the load-bearing capacity of the considered system.

By taking into account the fact that the external load having an impact on the entire system is carried by both the supported and supporting system, there are limits in the applicability of the presented results. The first limitation is the strength of the supported system, strictly connected with its stiffness. The second limiting factor of applicability of the results is the boundary of proportionality, which is under the large influence of temperature of the column subjected to heating.

The structure exposed to a higher temperature (e.g. during a fire) decreases its load-bearing capacity, and, in turn, directly influences the danger of losing one's health or even life. The time from the moment of heating occurrence (e.g. initiation of fire) until the moment where the load-bearing capacity of the system decreases to a dangerous level due to heating is very significant and should be as long as possible. The extension of time allows evacuation of the people and to protect property in the event of danger regarding the destruction of the supporting structure.

The research, the results of which are presented in this paper, should be continued for two reasons. The first – to provide the constructors of supporting systems with greater knowledge on what happens with the structure that will be heated. On the other hand, this type of research should be conducted in order to determine the way to extend the durability of the structure when it becomes exposed to high temperature.

## ACKNOWLEDGEMENT

This study was carried out within the statutory fund of the Czestochowa University of Technology (BS/PB 1-100-3010/2019/P).

## REFERENCES

[1] Timoshenko S, Gere JM. Theory of elastic stability. New York: McGraw-Hill; 1961.

[2] Tomski L, Uzny S. Vibration and stability of geometrically nonlinear column subjected to generalized load with a force directed toward the positive pole. International Journal of Structural Stability and Dynamics 2008;8(1):1–24.

[3] Uzny S. Free vibrations of an elastically supported geometrically nonlinear column subjected to a generalized load with a force directed toward the positive pole. Journal of Engineering Mechanics 2011;137(11):740–8.

[4] Tomski L, Uzny S. Free vibrations and the stability of a geometrically non-linear column loaded by a follower force directed towards the positive pole. International Journal of Solids and Structures 2008;45(1):87–112.

[5] Tomski L, Szmidla J, Uzny S. Active and passive specific loads with respect to the stability and free vibrations of columns. Journal of Engineering Mechanics 2014;140(1):193–205.

[6] CEN. Eurocode 3: Design of steel structures - Part 1-1: General rules and rules for buildings. 2005.

[7] Kiani Y, Eslami MR. Thermal buckling analysis of functionally graded material beams. International Journal of Mechanics and Materials in Design 2010;6(3):229–38.

[8] Liu L, Kardomateas GA, Birman V, Holmses JW, Simitses GJ. Thermal buckling of a heat-exposed, axially restrained composite column. Composites Part A: Applied Science and Manufacturing 2006;37(7):972–80.

[9] Shepherd PG, Burgess IW. On the buckling of axially restrained steel columns in fire. Engineering Structures 2011;33(10):2832–8.

[10] Wang WY, Li GQ. Fire-resistance study of restrained steel columns with partial damage to fire protection. Fire Safety Journal 2009;44(8):1088–94.

[11] Li GQ, Wang WY, Chen SW. A simple approach for modeling fire-resistance of steel columns with locally damaged fire protection. Engineering Structures 2009;31(3):617–22.

[12] Tan KH, Yuan WF. Buckling of elastically restrained steel columns under longitudinal non-uniform temperature distribution. Journal of Constructional Steel Research 2008;64(1):51–61.

[13] Tan KH, Yuan WF. Inelastic buckling of pin-ended steel columns under longitudinal non-uniform temperature distribution. Journal of Constructional Steel Research 2009;65(1):132–41.

[14] Cai JG, Feng J, Zhang J. Thermoelastic buckling of steel columns with load-dependent supports. International Journal of Non-Linear Mechanics 2012;47(4):8–15.

[15] Fu Y, Wang J, Hu S. Analytical solutions of thermal buckling and postbuckling of symmetric laminated composite beams with various boundary conditions. Acta Mechanica 2014;225(1):13–29.

[16] Dwaikat MMS, Kodur VKR, Quiel SE, Garlock MEM. Experimental behavior of steel beam-columns subjected to fire-induced thermal gradients. Journal of Constructional Steel Research 2011;67(1):30–8.

[17] Yang KC, Lee HH, Chan A. Performance of steel H columns loaded under uniform temperature. Journal of Constructional Steel Research 2006;62(3):262–70.

[18] Lienhard IV JH, Lienhard V JH. A heat transfer textbook. 5th ed. Mineola, New York: Dover Publications; 2019.

[19] Ancas A, Grobanescu D. Theoretical models in the study of temperature effect on steel mechanical properties. Bulletin of the Polytechnic Institute of Jassy, Construction. Architecture Section 2006;52(1–2):49–54.

[20] Burden RL, Faires JD. Numerical analysis. 9th ed. Boston, MA: Brooks/Cole, Cengage Learning; 2011.